



Preparation of aluminum–ferric–magnesium polysilicate and its application on oily sludge

SI LI, SHUANG-CHUN YANG*, YI PAN and JIN-HUI ZHANG

Liaoning Shihua University, FuShun 113001, China

(Received 29 December 2014, revised 9 March, accepted 17 March 2015)

Abstract: Aluminum–ferric–magnesium polysilicate (PAFMS) was prepared by introducing aluminum, ferric and magnesium metal ions into polysilicon acid solution. In this study, PAFMS was applied in the treatment of oily wastewater from the treatment of oily sludge, and the coagulation performance was evaluated by the efficiency of the removal of turbidity and color. The structure and morphology of PAFMS were characterized by Fourier transform infrared spectroscopy (FTIR), X-ray diffraction (XRD) and scanning electronic microscopy (SEM). The results indicated that the mole ratio 6:4:15 of Al:Fe:Mg is beneficial to the formation of Al–O–Si, Fe–O–Si and Mg–Si–O. Fe played the main inhibition role among the three metals. XRD analysis showed that the addition of Al, Fe and Mg into polysilicic acid did not produce a simple mixture, but resulted in the formation of new chemical structures. The intensity of peaks was influenced by the mole ratios of metals. SEM showed that PAFMS appeared to be a spatial structure consisting of many irregular protuberant parts. The removal efficiency of turbidity and color in oily water from the treatment of oily sludge was better when the mole ratio of (Al+Fe+Mg):Si was 0.5 and if the mole ratios of Al:Fe:Mg are kept at 6:4:15. Moreover, when the dosage of PAFMS was 1.4–1.8 % and the pH value in range of 8–9, the efficiency of turbidity and color removal were up to 97.3 and 96.8 %, respectively.

Keywords: coagulation; flocculants; aluminum–ferric–magnesium polysilicate; oily sludge; magnesium; inorganic polymer.

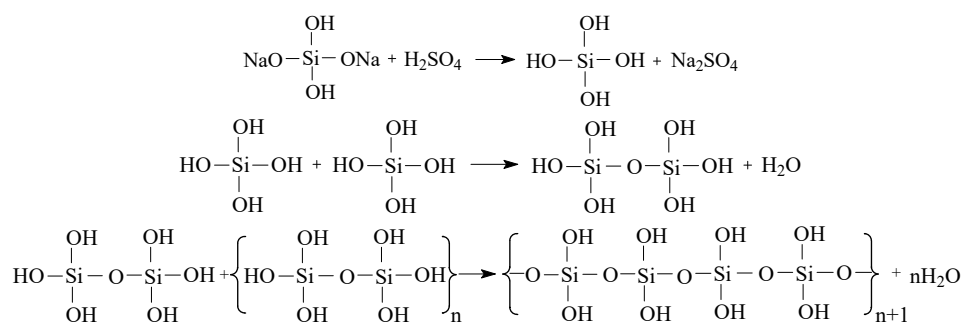
INTRODUCTION

Coagulation is one of the important steps in the water and wastewater treatment process. Flocculants could be divided into two categories: organic and inorganic. Organic polymer flocculants, which can exert perfect flocculation effect at small dose, are expensive and toxic. However, inorganic flocculants are cheaper and wider applied. Polysilicic acid (PSi), which was synthesized in 1937, is difficult to store because of its poor stability.¹ Metals flocculants have the bad

* Corresponding author. E-mail: yangchun_bj@126.com
doi: 10.2298/JSC141229057L

effect of coagulation at low temperatures. This is because the hydrolysis reaction is difficult under low temperatures, however, the floc of metal flocculants mainly rely on the hydrolysis reaction. Furthermore, metallic residues will be present in the effluent from water treated by metals flocculants. Hence, metal polysilicate flocculants were developed to address this issue; they can unite the features of PSi and metals to exert charge neutralization, adsorption bridging and network capturing. In recent years, metal polysilicate flocculants have been the focus of research into inorganic flocculants.^{2–4}

Silicic acid monomers can be isolated when strong acid is added into a Na₂SiO₄ solution and PSi formation follows in the condensation polymerization of monomeric silicic acid.⁵ The mechanism is as follows:



At higher degrees of polymerization, PSi gels and loses its flocculation effect. However, metals can prevent the gelation of PSi by reacting with the –OH on the PSi chain ends. In addition, metals supply positive charges to the PSi surface, which make PSi capable of “charge neutralization” and “network capturing”.⁶

Flocculants with aluminum ions produce larger but looser flocs that are difficult to settle. There is also the possibility of biologically toxic residual Al in the treated water. Ferric ions can make the flocs more compact and easy to settle, but the color of the effluent is pronounced.⁷ However, magnesium ions can play a decolorizing role because they can create insoluble complexes (for example, MgHN₃PO₄·6H₂O).⁸ Magnesium can reduce the Al³⁺ and Fe³⁺ residuals.⁹ Al polysilicate and Fe polysilicate were investigated in many studies,^{10–13} but there are only a few studies about magnesium-containing flocculants. Yanjie¹⁴ prepared ferric–magnesium polysilicate (PSIFM) by copolymerization, and its removal for COD (chemical oxygen demand) and SS (suspended substances) was found to be up to 80 and 90 %, respectively. Polysilic aluminum–magnesium sulfate was prepared and applied in the treatment of oily wastewater by Tianbin *et al.*,¹⁵ and its maximum turbidity removal can reach 97.6 %.

Oily sludge is one of the main pollutants in the petrochemical industry. It is a key factor constraining the improvement of the environmental quality in oil-

fields.¹⁶ It has a complex composition and is difficult to treat. The hot washing method was a widely used method for oily sludge treatment. The reagents used in the hot washing method included surfactants, sodas and flocculants. Flocculants play the role of turbidity removal and dewatering. The development of flocculants has a very important significance for the hot washing method of oily sludge treatment. Oily sludge can be separated into three phases, oil, sludge and water, because of de-emulsification by the addition of a hot soda or surfactant solution. However, the aqueous phase still has a high turbidity.¹⁷ Thus, in this paper, the aqueous phase from oily sludge treatment with Tween 80 was used as the object to be treated.

The subject of this study was to prepare aluminum–ferric–magnesium polysilicate (PAFMS), a new type of polysilicate coagulant, by introducing aluminum, ferric and magnesium ions into polysilicic acid. The preparation and application conditions were optimized in terms of the removal of turbidity and color from oily wastewater obtained by phase separation of oily sludge. Finally, the PAFMS powders were characterized by FTIR spectroscopy, XRD analysis and SEM.

EXPERIMENTAL

Wastewater samples

The oily sludge used in these experiments was tank sludge obtained from the Liaohe Oilfield of CNPC, China. Its water content was 33.9 %, the oil content was 11.4 % and the sand content was 54.7 %. It was treated by the hot washing method using Tween 80 under the following conditions: temperature, 60 °C and a solid–liquid ratio of 1:6. The oily wastewater, the water phase obtained from oily sludge treatment, was the subject of further experiments.

Preparation of flocculants

PAFMS was prepared by co-polymerization (hydroxylation of a mixture of Al^{3+} , Fe^{3+} and Mg^{2+} and fresh polysilicic acid (PSi)). The following solutions were prepared: 0.5 mol L⁻¹ Na_2SiO_4 , 0.233 mol L⁻¹ H_2SO_4 , 0.5 mol L⁻¹ AlCl_3 , 0.5 mol L⁻¹ $\text{Fe}_2(\text{SO}_4)_3$ and 0.5 mol L⁻¹ MgCl_2 . The pH of 10 mL Na_2SiO_4 solution was adjusted to 5.5 with dilute sulfuric acid.¹⁸ The mixture of Na_2SiO_4 solution and dilute sulfuric acid was stirred until a pale blue appeared color. The “pale blue” implied the beginning of polymerization of the silicic acid monomers. The pale blue solution was fresh PSi. Three metal salts solution of different volumes were mixed to form mixed metal solution at different metal mole ratios. Finally, fresh PSi was poured into mixed metal solution. Then mixed solution was stirred constantly and then aged.

Batch coagulation–flocculation test

The pH of wastewater was adjusted to 9 by adding NaOH. The wastewater with appropriate amount of PAFMS was stirred rapidly at 180 rpm for 2 min, and then slowly at 60 rpm for 10 min. Wastewater after treatment was left to precipitate for 30 min.

According to GB13200-91 (Chinese National Standard),¹⁹ the turbidity was measured at a wavelength of 680 nm. The turbidity removal efficiency (*RE*) was calculated as follows:

$$TRE = 100 \frac{T_0 - T_i}{T_0} \quad (1)$$

where T_0 is the turbidity of the wastewater and T_i is the turbidity of the wastewater after treatment.

The absorption peaks of wastewater were determined for the analysis of wastewater color by scanning the wavelengths from 280 to 500 nm. The highest absorption peak appeared at 482 nm. The color removal efficiency (*CRE*) was calculated using the absorbance at 482 nm by applying Eq. (2):

$$CRE = 100 \frac{A_0 - A_i}{A_0} \quad (2)$$

where A_0 is the absorbance of the wastewater and A_i is the absorbance of the wastewater after treatment.

Characterization

The liquid samples of PAFMS were dried at 50 °C for 10 h and then placed in a desiccator to cool to room temperature. The solid PAFMS was ground for the further characterization studies. The chemical bonds in PAFMS were analyzed by Fourier transform infrared spectroscopy using the KBr pellet method. The spectra were recorded in the range 400–4000 cm⁻¹ at a scan resolution of 2 cm⁻¹. X-Ray diffraction analysis was applied for the determination of crystalline phases in the solid PAFMS using a D/MAX-RB X-ray diffractometer with CuK α radiation in the 2θ range 10–70° at a scan rate of 8° min⁻¹. The morphology was determined by scanning electron microscopy (SEM) at an acceleration voltage of 30 kV and a magnification of 1000 \times .

RESULTS AND DISCUSSION

The optimization of metal ratio

The optimal mole ratios of Al:Fe:Mg and (Al+Fe+Mg):Si were determined and the results are shown in Figs. 1–3.

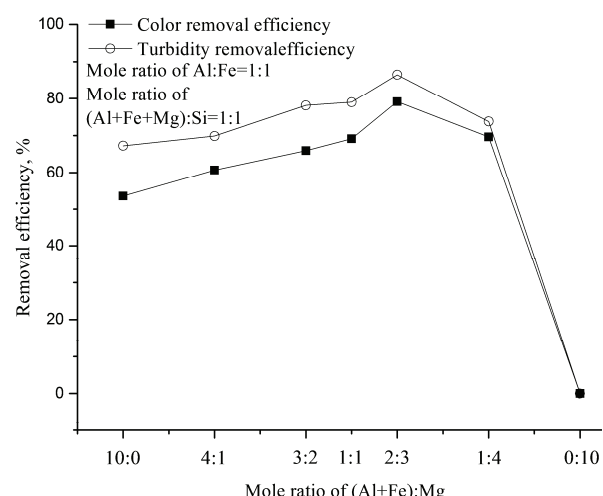


Fig. 1. Effect of the volume of MgCl₂ solution (V_{MgCl_2}) on the coagulation performance.

The changes in the removal efficiency when the mole ratios of (Al+Fe): Mg were 10:0, 4:1, 3:2, 1:1, 2:3, 1:4 and 0:10 are indicated in Fig 1. Before the

maximum removal efficiencies of turbidity and color were achieved, the removal efficiencies increased with increasing mole ratio of Mg. This illustrates that Mg^{2+} improves the coagulation performance and the decolorizing function of PAFMS. The optimum mole ratio of (Al+Fe):Mg was 2:3. After this maximum, further increases in the amount of Mg^{2+} would result in decreased removal efficiencies of turbidity and color. There are two reasons for this decrease in removal efficiency First Mg^{2+} has less positive charges than Al^{3+} and Fe^{3+} . Once the mole ratio of (Al+Fe):Mg exceeds 2:3, the overall charges on the PAFMS would decrease resulting in a weak charge neutralization function of PAFMS. The second reason is Mg^{2+} has smaller molecular mass than Al^{3+} and Fe^{3+} . When mole ratios of (Al+Fe):Mg exceeded 2:3, the settlement velocity would become slow leading to a decrease in the removal efficiency. From Fig. 1, it can be seen that when only Mg^{2+} was added into PSi ((Al+Fe):Mg mole ratio is 0:10), the removal efficiency was 0. This is because PAFMS gelled rapidly to lose the flocculant function in coagulation process, which implies Mg cannot effectively inhibit the gelation of PSi.

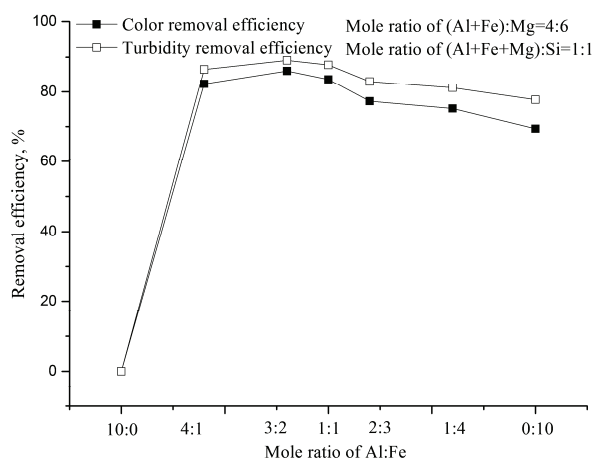


Fig. 2. Effect of volume of $Fe_2(SO_4)_3$ solution ($V_{Fe_2(SO_4)_3}$) on the coagulation performance.

The removal efficiencies of turbidity and color when the mole ratios of Al:Fe were 10:0, 4:1, 3:2, 1:1, 2:3, 1:4 and 0:10 are shown in Fig. 2. The removal efficiency was zero when no Fe^{3+} (Al:Fe mole ratio 10:0) was added to the PSi, which illustrates Fe plays the main inhibition role among the three kinds of metals (Fe, Al and Mg). With the increasing amount of Fe^{3+} , the removal efficiency gradually achieved its maximum value, and then started to decrease. The maximum removal efficiency appeared when mole ratio of Al:Fe was 3:2. The reason of decreasing removal efficiency of turbidity is that the settlement velocity of PAFMS could be accelerated with the increasing amount of Fe, which has a larger molecular weight than Al.²⁰ On the other hand, Fe^{3+} has color and its

floc is smaller than that of Al^{3+} , and a mole ratio of Al: Fe exceeding 2:3 lead to decreasing color removal efficiency. According to the results shown in Figs. 1 and 2, the favorable mole ratio of Al:Fe:Mg is 6:4:15.

The changes in removal efficiencies when the mole ratios of $(\text{Al}+\text{Fe}+\text{Mg})\text{:Si}$ were 0.25:1, 0.5:1, 0.75:1, 1:1, 1.25:1, 1.5:1 and 2:1 are displayed in Fig. 3. The optimum value of the mole ratio of $(\text{Al}+\text{Fe}+\text{Mg})\text{:Si}$ was 0.5. Before the removal efficiency achieved the maximum, the removal efficiency increased with the increasing of content of $(\text{Al}+\text{Fe}+\text{Mg})$. After this maximum, with continuing increases in the amount of metals, the removal efficiencies decreased. Before the optimal mole ratio, the charge of PAFMS increased because of the increasing mole ratio of $(\text{Al}+\text{Fe}+\text{Mg})\text{:Si}$, which led to a better charge neutralization function. After the optimal mole ratio, the adsorption bridging function of PAFMS was weakened by the decreasing amount of Si.

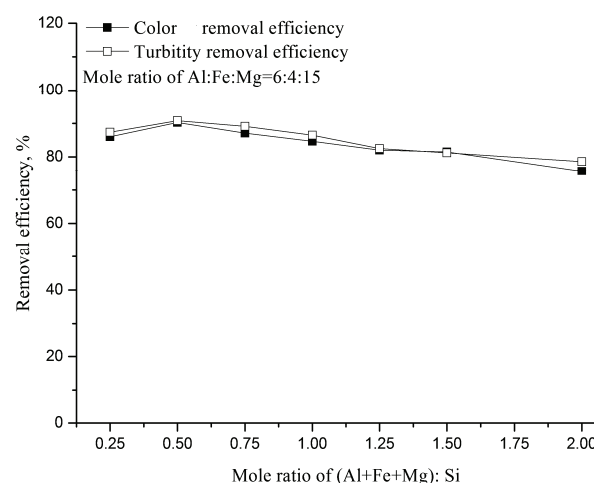


Fig. 3. Effect of mole ratio of $(\text{Al}+\text{Fe}+\text{Mg})\text{:Si}$ on the coagulation performance.

Effect of PAFMS dosage on coagulation performance

The changes in the removal efficiencies when the PAFMS dosages were 0.5, 1.0, 1.4, 1.6, 1.8, 2.0 and 3.0 % are shown in Fig. 4. The optimum value for the PAFMS dosage was 1.6 %, however, the removal efficiency was always more than 85.0 % when the PAFMS dosage was within the range 1.4–1.8 %. Before the removal efficiency achieved its maximum value, the removal efficiency increased with increasing PAFMS dosage. After this maximum, a continuing increase in the PAFMS dosage resulted in decreased removal efficiency. When the dosage of PAFMS exceeded 2.0 %, because the positive charges from PAFMS adhered around the suspended matter in the wastewater and the native charges on suspended matters became positive. This made the suspension of the matter in

the wastewater stable. For this reason, the removal efficiency decreased. Thus, the dosage of PAFMS should lie in the range 1.4 %–1.8 % to avoid higher costs.

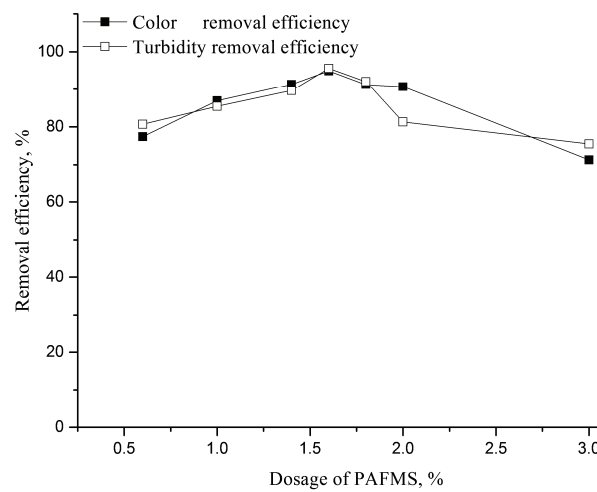


Fig. 4. Effect of PAFMS dosage on the coagulation performance.

Effect of pH of oily wastewater on coagulation performance

The changes in the removal efficiencies when the pH values of the wastewater were set at 7, 8, 9, 10 and 11 are shown in Fig. 5. With increasing pH value, the removal efficiency gradually achieved its maximum value, and then started to decrease. When the pH value was in the range 8–9, the maximum efficiency of turbidity removal and color removal were 97.3 % and 96.8 %, respectively. In this pH range, Al^{3+} , Fe^{3+} and Mg^{2+} have rich variety of hydrolysates

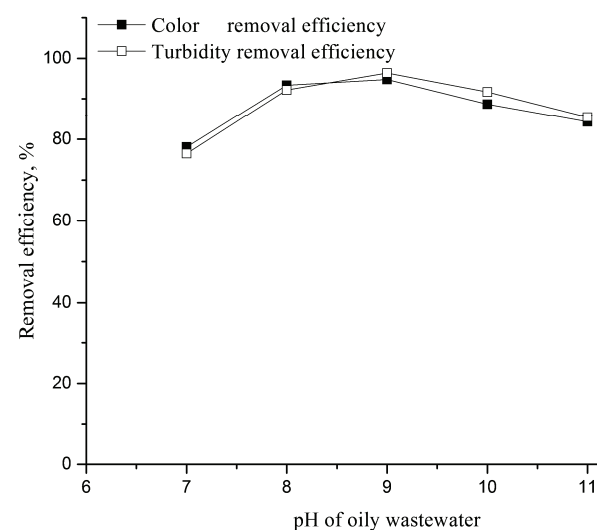


Fig. 5. Effect of the pH of the oily wastewater on coagulation performance.

and hence a large amount of polynuclear complexes and hydroxy complex ions²¹ are generated, leading to improved adsorption bridging and network capturing functions by PAFMS. Furthermore, PAFMS exhibited a positive potential, but the suspended matters has a negative potential. This illustrates that a pH value in the range 8–9 is the best range for charge neutralization. However, when the pH value exceeded 9, the degree of dissociation of PSi was too large²² for PSi exhibit an adsorption bridging function.

Characterization of the PAFMS

FTIR analysis. The FTIR spectrum of PSi is shown in Fig. 6a, while the FTIR spectra of PAFMS with different mole ratios of the metals are presented in Fig. 6b–d. In Fig. 6b, the mole ratio of Al:Fe:Mg was 6:4:15, and (Al+Fe+Mg):Si ratio was 0.5:1, *i.e.*, it shows the spectrum of the PAFMS with the optimal metal ratios. In Fig. 6c, the mole ratio of (Al+Fe):Mg was 4:1, and (Al+Fe+Mg):Si was 1:1, *i.e.*, it shows the spectrum of the PAFMS with a lower amount of Mg²⁺. In Fig. 6d, the mole ratio of Al:Fe:Mg was 6:4:15, and (Al+Fe+Mg):Si was 1.5:1, *i.e.*, it shows the spectrum of the PAFMS with an excessive amount of (Al+Fe+Mg).

In Fig. 6b–d, characteristics peaks at 3700–3900 cm^{−1} could be attributed to the symmetric and antisymmetric stretching of M–OH (Al–OH, Fe–OH and Mg–OH).²³ This peak does not appear in Fig. 6a, which indicated that the metals had reacted with the –OH on the PSi chain ends. Intensity of peaks in Fig. 6b and d are stronger than those in Fig. 6c. This illustrates that Mg²⁺ is better for the formation of M–OH bonds.

The peaks at 3500–3300 cm^{−1} were assigned to the stretching vibration of –OH.²⁴ In Fig. 6b and d, there are shoulder peaks around 3500–3300 cm^{−1} and peak area is larger than in Fig. 6a. This implies that the amount of –OH increased. This phenomenon could be attributed to an increase in absorbed water and –OH linked with Al³⁺, Fe³⁺ and Mg²⁺.

The peaks at 1660–1640 cm^{−1} corresponded to bending vibrations of H–O–H, which implies all four samples were hydroxyl polymers²⁵. There is a strong absorption peak at 1099.9 cm^{−1} in the spectrum presented in Fig. 6a, which could be attributed to the stretching vibration of Si–O–Si groups, which arose because of the condensation polymerization of silicic acid monomers. However, all Si–O–Si peaks shown in Fig. 6b–d are weaker than in Fig. 6a, and blue-shifted to 1150.5, 1105.5 and 1139.2 cm^{−1}, respectively. Peaks at 1150.5, 1105.5 and 1139.2 cm^{−1} are assigned to the characteristics peaks of Al–OH–Al, Fe–OH–Fe and Mg–OH–Fe, respectively. This proves that metals can prevent the gelation of PSi. This corresponds to the research results of Yuemei.²⁶ There is another possibility, the peaks around 1100 cm^{−1} could also be attributed to the characteristics peaks of SO₄^{2−}. From Fig. 6a–d, it could be seen that the peaks around 1100 cm^{−1} of Fig. 6a are stronger than those of Figs. 6b–d (at 1150.5,

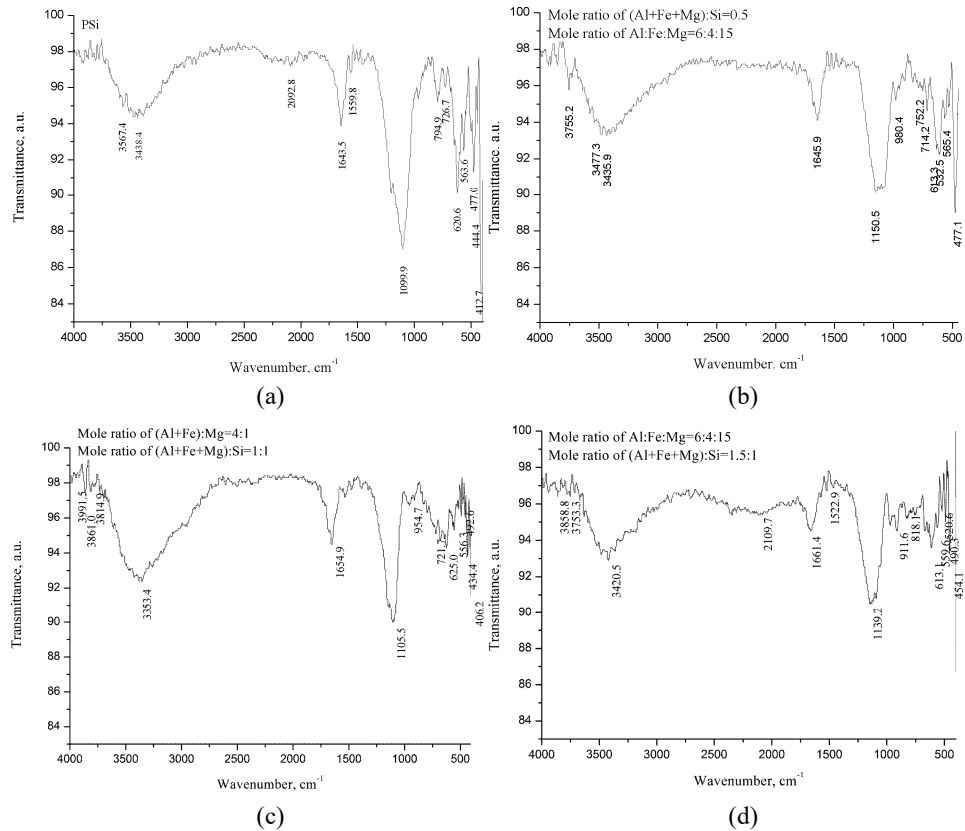


Fig. 6. FTIR spectra of PSi and PAFMS with different mole ratios of metals: a – PSi; b – PAFMS prepared under mole ratio of $(\text{Al}+\text{Fe}+\text{Mg})\text{:Si} = 0.5$, mole ratio of $\text{Al}\text{:Fe}\text{:Mg} = 6\text{:4:15}$; c – PAFMS prepared under mole ratio of $(\text{Al}+\text{Fe}+\text{Mg})\text{:Si} = 0.5$, mole ratio of $(\text{Al}+\text{Fe})\text{:Mg} = 4\text{:1}$; d – PAFMS prepared under mole ratio of $(\text{Al}+\text{Fe}+\text{Mg})\text{:Si} = 1.5$, mole ratio of $\text{Al}\text{:Fe}\text{:Mg} = 6\text{:4:15}$.

1105.5 and 1139.2 cm^{-1} , respectively). This indicates SO_4^{2-} would coordinate with metal ions and participate in the polymerization when metal salts were added into PSi.²⁷

Characteristic peaks at 910–960 cm^{-1} in Figs. 6b–d could be attributed to the stretching vibration of $\text{Al}-\text{O}-\text{Si}$ and $\text{Fe}-\text{O}-\text{Si}$.¹⁴ The intensity of this peak is closely related to the coagulation performance. The peak intensity at 960.4 cm^{-1} in Fig. 6b is the strongest. The peak at 532.5 cm^{-1} in Fig. 6b and the peak at 520.6 cm^{-1} in Fig. 6d were assigned to the stretching vibration of $\text{Si}-\text{O}-\text{Mg}$,²⁵ but they did not appear in Fig. 6c. This implies that greater amount of Mg would form more $\text{Si}-\text{O}-\text{Mg}$ groups. In a word, the generation of $\text{Al}-\text{O}-\text{Si}$, $\text{Fe}-\text{O}-\text{Si}$ and $\text{Mg}-\text{O}-\text{Si}$ indicate the metals had polymerized with PSi. The peak at 794.0 cm^{-1}

in Fig. 6a, assigned to the connection of tetrahedron of Si–O–Si,²⁵ did not appear in Figs. 6b–d. This indicates PAFMS has a reticular formation.

In conclusion, FTIR analysis supports the formation of new chemical species of PAFMS consisting of aluminum, iron, magnesium and silica.

XRD analysis

Figure 7 illustrates The XRD patterns of PSi and PAFMS with different mole ratios of metals are illustrated in Fig. 7.

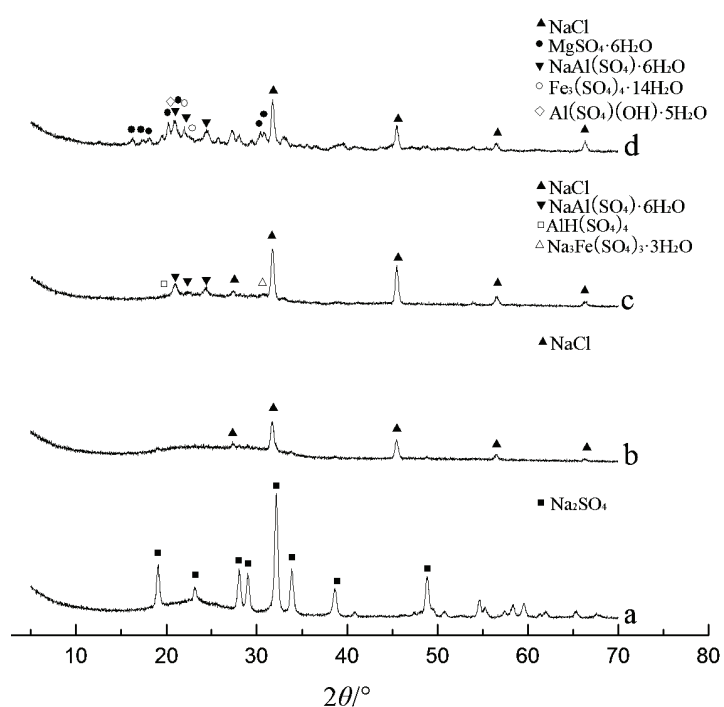


Fig. 7. XRD spectra of PSi and PAFMS with different mole ratios of metals: a – PSi; b – PAFMS prepared under mole ratio of (Al+Fe+Mg):Si = 0.5, mole ratio of Al:Fe:Mg = 6:4:15; c – PAFMS prepared under mole ratio of (Al+Fe+Mg):Si = 0.5, mole ratio of (Al+Fe):Mg = 4:1; d – PAFMS prepared under mole ratio of (Al+Fe+Mg):Si=1.5, mole ratio of Al:Fe:Mg = 6:4:15.

The XRD spectrum of PSi has clear diffraction peaks, but the spectra of PAFMS have no diffraction peaks. With the introduction of metal ions, the intensity of peaks was weakened and the width of peaks was broadened. There is a diffuse peak group, which indicates PAFMS is a new type of multipolymer without fixed regular structures; it is a kind of macromolecule with long-range disorderly structures. Diffraction crystal peaks of Na₂SO₄ (at 2θ 19.035, 23.153, 28.027, 28.990, 32.123, 33.826, 38.615 and 49.443°) were only found in the spectrum of

PSi, which implies the introduction of metals impelled SO_4^{2-} to participate in the copolymerization. This corresponds to the results of the FTIR analysis.

Crystal peaks NaCl (at 2θ 27.334, 31.692, 45.449, 56.477 and 66.227°) appeared in the patterns of the PAFMS samples (Fig. 7, b-d), which illustrates Cl^- did not fully participate in the polymerization reaction. The intensity of NaCl crystal peaks in Fig. 7, c, were stronger than in Fig. 7, b and d, which implies that the increasing amount of Mg^{2+} could promote Cl^- to polymerize with PSi.

Polymerization between metals and PSi could produce an amorphous substance and hence, the more complete is the polymerization reaction, the smoother is the amorphous peak groups at 2θ 18–30°. Obviously, the peak shape in Fig. 7, b, is more regular, and the amorphous peak groups at 2θ 18–30° is smoother. This indicates the PAFMS had a better coagulation performance with more amorphous substance.

Crystal peaks of metal ions were observed in Fig. 7, d, *i.e.*, $\text{MgSO}_4 \cdot 6\text{H}_2\text{O}$ (at 2θ 16.250, 17.688, 18.164, 20.211, 21.983, 24.640, 30.084 and 30.367°), $\text{NaAl}(\text{SO}_4)_2 \cdot 6\text{H}_2\text{O}$ (at 2θ 21.034, 24.366 and 30.818°) and $\text{Fe}_3(\text{SO}_4)_4 \cdot 14\text{H}_2\text{O}$ (at 2θ 21.950 and 22.336°), which indicates that excessive metals do not participate in the polymerization reaction.

Diffraction patterns of crystals, such as AlCl_3 , $\text{Fe}_2(\text{SO}_4)_3$, MgCl_2 , Al_2O_3 , Fe_2O_3 , Fe_3O_4 , MgO , $\text{Al}(\text{OH})_3$, $\text{Fe}(\text{OH})_3$, $\text{Mg}(\text{OH})_3$ and SiO_2 were not observed in Fig. 7, b, which confirms that the metal ions had polymerized with PSi. Amorphous or new compounds were formed in PAFMS. The XRD analysis shows that the addition of Al^{3+} , Fe^{3+} and Mg^{2+} did not produce a simple mixture in PSi, but resulted in the formation of new chemical structures. The intensity of the peaks was influenced by the mole ratios of the metals.

SEM micrography

The surface morphology of PAFMS powder with optimal metal ratios, which is a reticular formation consisting of many irregular and non-direction protuberant parts, is presented in Fig. 8. This corresponds to the results of FTIR analysis. A series of holes of different width and depth are distributed, which indicates PAFMS presents a large surface area. The reasons for the formation of this structure is that metal ions adsorbed or polymerized with the –OH at the ends of PSi.

CONCLUSIONS

A new inorganic coagulant PAFMS was prepared in this study, the mole ratios of metals and application conditions were optimized. The structure and surface characteristics of PAFMS were analyzed by FTIR, XRD and SEM.

As the experiment results showed, the characteristics of PAFMS were largely affected by the mole ratios of metals. Removal efficiency was maximal when the

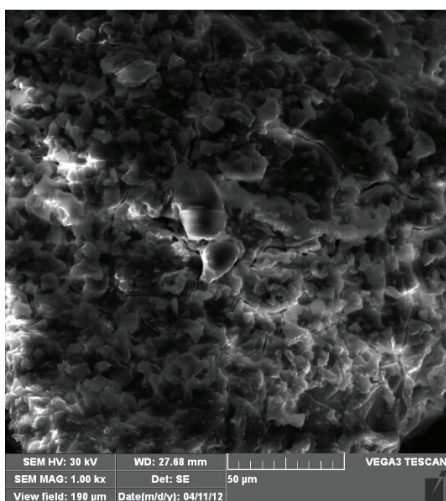


Fig. 8. SEM image of PAFMS.

mole ratio of (Al+Fe+Mg):Si was 0.5 and the mole ratio of Al:Fe:Mg was 6:4:15. Moreover, when the dosage of PAFMS was 1.6 % and wastewater pH value in range of 8–9, the removal efficiency of turbidity and color were up to 97.3 % and 96.8 %, respectively. The results of the FTIR analysis indicated that there were bonds formed by polymerization between metals and PSi in PAFMS, such as Al–OH, Fe–OH, Mg–OH, Al–OH–Al, Fe–OH–Fe, Mg–OH–Mg, Al–O–Si, Fe–O–Si and Mg–Si–O. Moreover, the intensities of the FTIR peaks were influenced by the mole ratios of the metals. In XRD patterns of PAFMS, there was an amorphous group of peaks at 2θ 18–30°. This implies PAFMS is a kind of amorphous multipolymer with no regular structure. The peak shape in XRD spectra of PAFMS under optimal conditions was more regular. Meanwhile, in SEM microphotograph, PAFMS showed a reticular formation consisting of many irregular protuberant parts. In conclusion, as a new type inorganic flocculant, PAFMS has further research value.

Acknowledgements. This work was supported by the Project of Liaoning Provincial Industrial Magnesium Resources Protection Office (The synthesis and application of magnesium-based polymeric flocculants) and Training Programs of Innovation and Entrepreneurship for Undergraduates of Liaoning Provincial (Research and development of composite flocculant special for acrylic fiber wastewater).

И З В О Д
СПРАВЉАЊЕ АЛУМИНИЈУМ–ФЕРИ–МАГНЕЗИЈУМ–ПОЛИСИЛИКАТА И ЊЕГОВА
ПРИМЕНА НА НАФТНОМ МУЉУ

SI LI, SHUANG-CHUN YANG, YI PAN и JIN-HUI ZHANG

Liaoning Shihua University, FuShun 113001, China

Поли-алуминијум–фери–магнезијум–силикат (PAMFC) је справљен уношењем јона метала алуминијума, гвожђа и магнезијума у кисели раствор. Учинак коагулације је

оцењиван уклањањем мутноће и обоења отпадне воде од третмана нафтног муља. Структура и морфологија PAMFC су карактерисане инфрацрвеном спектроскопијом са Фурије трансформацијом (FTIR), рентгенском дифракцијом (XRD) и сканирајућом електронском микроскопијом (SEM). Резултати су указали да је однос 6:4:15 метала Al:Fe:Mg погодан за формирање Al-O-Si, Fe-O-Si и Mg-Si-O. Од ова три метала, гвожђе је највише играло улогу инхибитора. XRD анализа је показала да додатак Al, Fe и Mg у полимерну силицијумову киселину доводи до формирања нове хемијске врсте, а не обичне смеше. Интензитет пикова је зависио од молских фракција метала. Према SEM, PAMFC се показао као просторна структура која се састоји од много неправилних истурених делова. Када је молски однос (Al+Fe+Mg):Si био 0,5, а Al:Fe:Mg на 6:4:15, ефекат уклањања је био бољи. Штавише, када је дозирање PAMFC било 1,4–1,8 % или 8–9 %, тада је уклањање мутноће и обоења било 97,31, односно 96,76 %.

(Примљено 29. децембра 2014, ревидирано 9. марта, прихваћено 17. марта 2015)

REFERENCES

1. S. L. Yu, L. Liu, X. Y. Liu, *J. Harbin. Univ. Civil Eng. Arch.* **30** (1997) 62 (in Chinese)
2. Z. L. Yang, B. Liu, B. Y. Gao, *Sep. Purif. Technol.* **111** (2013) 119
3. Z. M. Qiu, W. T. Jiang, Z. J. He, *J. Hazard. Mater.* **166** (2009) 740
4. G. C. Zhu, H. L. Zheng, W. Y. Chen, W. Fan, P. Zhang, T. Tshukudu, *Desalination* **285** (2012) 315
5. S. L. Yu, X. Y. Liu, L. Liu, *J. Harbin. Univ. Civ. Eng. Arch.* **29** (1996) 111 (in Chinese)
6. X. Xu, S. L. Yu, W. X. Shi, *Sep. Purif. Technol.* **66** (2009) 486
7. C. J. Wang, N. Y. Gao, S. J. Zhao, *Sichuan Environ.* **28** (2009) 119 (in Chinese)
8. J. X. Zhang, J. R. Lu, B. T. Shan, *Ind. Water Treat.* **8** (2009) 56 (in Chinese)
9. L. Chen, L. Sha, Z. H. Zhang, *Tech. Water Treat.* **37** (2011) 42 (in Chinese)
10. B. Y. Gao, Q. Y. Yue, Y. H. Song, *Environ. Chem.* **2** (1998) 170 (in Chinese)
11. H. Y. Yang, F. Y. Cui, Q. L. Zhao, *J. Zhejiang. Univ.: Sci.* **5** (2004) 721
12. Z. M. Lu, C. S. Wu, Y. J. Diao, *Guangzhou Chem.* **35** (2010) 28 (in Chinese)
13. W. B. Lv, X. L. Zhu, J. G. Li, *Pap. Sci. Technol.* **30** (2011) 86 (in Chinese)
14. Y. J. Wen, C. Y. Han, L. D. Zhang, *J. Beijing Univ. Chem. Technol. (Nat. Sci.)* **39** (2012) 90 (in Chinese)
15. T. B. Li, W. Chen, Y. B. Wan, *J. Yangtze Univ. (Nat. Sci. Ed.)* **8** (2011) 18 (in Chinese)
16. X. B. Li, J. T. Liu, Y. Q. Xiao, *J. Cent. South Univ. Technol.* **18** (2011) 367
17. B. C. A. Pinheiro, J. N. F. Holandan, *Ceram. Int.* **39** (2013) 57
18. Y. B. Duan, S. Z. Yi, *Environ. Prot. Chem. Ind.* **25** (2005) 239 (in Chinese)
19. GB13200-91, Water quality-Determination of turbidity (in Chinese)
20. Y. Fu, S. L. Yu, Y. Z. Yu, *J. Environ. Sci.* **19** (2007) 678
21. Y. Z. Li, *Shandong Chem. Ind.* **41** (2013) 51 (in Chinese)
22. G. Z. Zhu, *Pes. Ind.* **22** (2009) 28 (in Chinese)
23. H. Liu, Y. M. Fang, J. Shao, J. Liang, *Chem. Eng.* **127** (2006) 55 (in Chinese)
24. T. Song, C. H. Sun, G. L. Zhu, *Desalination* **268** (2011) 270
25. R. Li, C. He, Y. L. He, *Desalination* **319** (2013) 85
26. Y. M. Fang, *Ind. Safety Env. Prot.* **10** (2007) 22 (in Chinese)
27. K. Müller, G. Lefèvre, *Langmuir* **27** (2011) 6830.